Identification of Defects in Pipelines Through a Combination of FEM and ANN

A.N. Soloviev, Giang D.T. Nguen, P.V. Vasiliev and A.R. Alexiev

Abstract Defects identification method in the pipeline system is proposed. The method is based on a combination of finite element method (FEM) and artificial neural networks (ANNs). A finite element modeling of the monitoring system of the damaged state of the pipeline, which is a fragment of a pipe with a defect and piezoelectric actuators and sensors is carried out. The direct problem is reduced to initial boundary value problem of the theory of elasticity and electrodynamics. The inverse problem of identification of defects is reduced to the inverse geometrical problem. As additional information for the solution of inverse problems is the amplitude–time response (ATR) of electric potential on the free electrode sensors, the sensors were located before and after a defect, for measuring the reflected and transmitted acoustic waves excited by the actuators. Using this model, a set of direct problems is solved and a training set for the ANN is constructed. As the ANN architecture, we select a multilayer perceptron and back propagation learning algorithm is considered. The algorithm for the identification of defects contains several steps: (i) the location of a defect (determining the distance between the actuators and sensors and defect); (ii) determining the type of the defect (crack, volumetric defect); and (iii) the determination of the defect parameters (depth, slope of the crack, geometric parameters of the volume defect). A series of numerical experiments, in which the optimal ANN architecture, defined for each identification step, is performed.

A.N. Soloviev (✉) · P.V. Vasiliev
Don State Technical University, Rostov-on-Don, Russia
e-mail: solovievarc@gmail.com

A.N. Soloviev
I.I. Vorovich Institute of Mathematics, Mechanics and Computer Science,
Southern Federal University, Rostov-on-Don, Russia

G.D.T. Nguen
Viet Nam Maritime University, Hai Phong, Vietnam

A.R. Alexiev
Institute of Mechanics of Bulgarian Academy of Sciences, Sofia, Bulgaria

E.N. Barkanov et al. (eds.), *Non-destructive Testing and Repair of Pipelines*,
Engineering Materials, DOI 10.1007/978-3-319-56579-8_7

Keywords Identification · Crack · Defect · Finite element method (FEM) · Acoustic waves · Artificial neural network (ANN) · Inverse problems · Piezoactuator · Piezosensor · Amplitude–time response

1 Introduction

Reconstruction of defects in the pipeline caused by corrosion or by mechanical action is an important technical problem, the successful solution of which can prevent breakage of the pipes. Such identification may be carried out with instruments, which move along a pipeline and perform their monitoring. A more attractive way of detection is the use of acoustic sensors and receivers (piezoelectric transducer). They are mounted on a pipe and detect damage based on the reflected signals. Such a system should be equipped with software that allows us to identify the damage and its extent based on the analysis of the reflected or transmitted signal. Such software can be developed through the use of ANN [1]. Application of ANN in the problems of reconstruction of the damaged state of structural elements was described in works [2–8]. The use of different ANN architectures and algorithms was described in works [2–7]. Identification of defects in anisotropic plates by using ANN was present in work [8]. In work [4], the authors pointed out the advantages of identification methods that do not require the prior constructing of a mathematical model of the studied object.

In this paper, we developed a method of reconstruction of surface defects in pipes. Mathematically, the problem is reduced to the inverse geometrical problem of elasticity theory [9]. It is assumed that the defects locate on the outer or inner surfaces of the pipe and have axisymmetric configuration. Nonstationary acoustic signal is processed by actuator, located at some distance from the defect. The receiver locates there as well. The problem is solved in axisymmetric case using FEM. Finite element model of the pipeline track is built in the ANSYS. The signal (in the form of amplitude time response (ATR) of the radial and axial displacements) reflected from the defect is measured over time. The waves, reflected from the ends of the pipe segment, do not have time to come back to the receiver. In this way, the real conditions of an extended pipeline are modeled.

Analysis of the measured ATRs shows the possibility of their use in the inverse problems of identification of defects. The identification of defects may be carried out in two stages. At the first stage, the registration of a defect and the determination of the distance from the sensor to the defect are carried out. The problem of the first stage is solved on the base of the difference between the measured values of ATR for construction without defect and with the defect. Calculations show that the distance to the defect can be found using the signal arrival time, which is reflected by the defect. Thus, task of the first stage may be achieved by using hardware. The second stage provides the identification of the defect parameters (type, size, shape, volume, etc.). This task is much more difficult than the previous. Depending on the input information, it may have more than one solution. Artificial neural networks

are used as a tool for solving the inverse problem of the reconstruction of defects parameters. Artificial neural networks were originally designed for solving the problem of finding nonlinear dependencies. Unlike other algorithmic structures, there are not programmable, but trained on the data set, based on the different defect parameters. Training sets are constructed by solving direct problems in ANSYS. The trained network is able to correctly identify defect parameters. Input data for training ANN can be transformed by the FFT [10], which improves the identification process. The ANN architecture, ways of representing information, and the influence of defects sizes on the accuracy of the identification were studied in this chapter.

2 Formulation of Direct and Inverse Problems

2.1 Direct Problem

Formulation of direct problems is reduced to the initial boundary value problem of elasticity theory taking into account the energy dissipation adopted in finite element packages such as ANSYS, ACELAN, etc. The formulation consists of the following equations [11]:

$$\sigma_{ij,j} = \rho\ddot{u}_i + \rho\alpha\dot{u}_i, \quad i = 1, 2, 3 \tag{2.1}$$

$$\sigma_{ij} = c_{ijkl}(\varepsilon_{kl} + \beta\dot{\varepsilon}_{kl}). \tag{2.2}$$

$$\varepsilon_{kl} = \frac{1}{2}\left(u_{k,l} + u_{l,k}\right) \tag{2.3}$$

boundary conditions:

$$u_i|_{S_1} = u_i^0 \tag{2.4}$$

$$t_i = \sigma_{ij}n_j|_{S_k} = p_i \tag{2.5}$$

and initial conditions:

$$u_i|_{t=0} = g_i(x)\, \dot{u}_i|_{t=0} = v_i(x)\, x \in V_s. \tag{2.6}$$

Here ρ is the material density; u_i are the unknown components of the displacement vector; u_i^0, p_i are the known components of the displacement vector and surface loads; σ_{ij}, c_{ijkl} are the components of the stress tensor and elastic constants; s_k is the internal surface of the crack and the hole; and ε_{kl} are the components of the strain tensor. The factors α, β describe dissipative properties of the solid and are used in modern finite element analysis packages such as ANSYS, ABAQUS,

ACELAN, and so on. These factors are coupled with property of Q-linear oscillator through the following relationships [12]:

$$\alpha = \frac{2\pi f_{r1} f_{r2}}{Q(f_{r1} + f_{r2})}, \quad \beta = \zeta_d = \frac{1}{2\pi Q(f_{r1} + f_{r2})}, \tag{2.7}$$

where f_{r1} and f_{r2} are the first and second resonance frequencies, and Q is the quality factor.

The wave excitation and reception of the signal by using actuators and sensors, based on piezoelectric elements, are carried out. In this case, the linear theory of electrodynamics, taking into account the energy dissipation, is used. It is also taken into account in the ANSYS and ACELAN packages that

$$\rho \ddot{u}_i + \alpha \rho \dot{u}_i - \sigma_{ij,j} = f_i; \quad D_{i,i} = 0 \tag{2.8}$$

$$\sigma_{ij} = c_{ijkl}(\varepsilon_{kl} + \beta \dot{\varepsilon}_{kl}) - e_{ijk} E_k; \quad D_i + \varsigma_d \dot{D}_i = e_{ikl}(\varepsilon_{kl} + \varsigma_d \dot{\varepsilon}_{kl}) + \ni_{ik} E_k, \tag{2.9}$$

$$\varepsilon_{kl} = (u_{k,l} + u_{l,k})/2; \quad E_k = -\phi_k, \tag{2.10}$$

where f_i are the components of the vector of the density of mass forces; D_i are the components of the electric induction vector; e_{ijk} are the third-rank tensor components of piezomoduli; E_i are the components of the electric field vector; ϕ is the electric potential function; $\ni_{ij}$ are the second-rank components of the tensor of dielectric permittivity; and $\alpha, \beta, \varsigma_d$ are negative damping coefficients [12].

Among the electrical boundary conditions, we note the conditions on the electrodes of actuator S_a and on the sensor electrode S_e, which is connected to an external electric circuit, or free:

$$\varphi|_{S_a} = \varphi_0 f(t) \tag{2.11}$$

$$\int_{S_e} \dot{D}_n \mathrm{d}s = I, \tag{2.12}$$

where I is the current in the circuit (in the considered cases of free electrode it is equal to zero); φ_0 is the maximum value of the electric potential; and $f(t)$ is the function, describing the shape of the pulse (single step, used in the numerical results).

2.2 Inverse Problems

The inverse geometric problem of identification of cracks on the external or internal surface of the pipe is considered. The excitation of waves is carried out by the

piezoelectric actuator. As additional information, it used the ATR of electrical potential, measured by the piezoelectric sensors, disposed on the external surface of the pipe.

The solution of direct nonstationary problems for pipe fragment (Fig. 1, right) with a circular crack of depth dr (Fig. 1, left) on the outer or inner surface of the pipe is searched. Let h is the pipe length, r is the inner radius, tr is the thickness, s_1 is the distance between the first piezosensor and the defect, l_1 is the distance between the defect and edge of the pipe, s_2 is the distance from the piezoactuator to the second piezosensor, and l_2 is the distance from the second piezosensor to the edge of the pipe.

A fragment of pipe is considered, which in cylindrical coordinate system (r_*, θ, z_*) occupies an area $\Omega : r - \frac{tr}{2} \le r_* \le r + \frac{tr}{2},\ 0 \le \theta \le 2\pi,\ 0 \le z_* \le l$.

A system of differential equations, describing wave processes in the pipe Eqs. (2.1)–(2.3), is used. The lower edge plane $z_* = 0$ is fixed; the upper edge plane and the inner cylindrical surface are free of stresses; the outer surface of the pipe also is free of stresses, too. Crack faces do not interact with each other; so they are free from mechanical stresses, too. The initial conditions correspond to the non-deformed tube at rest. Dynamic processes in the electroelastic environment (piezoactuators and piezosensors) are described by Eqs. (2.8)–(2.10). On the electrodes of piezoactuator, a potential difference (2.11) is given. One electrode of the piezosensor, which gives information on ATR of electric potential (2.10), is

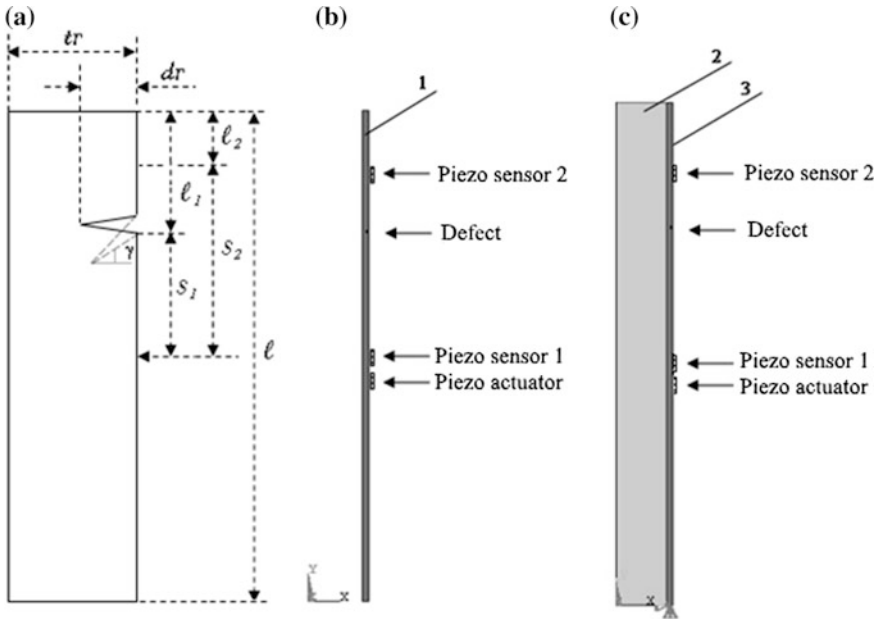

Fig. 1 **a** Pipe model with crack-like defect and shown dimensions; **b** pipe model without liquid; **c** pipe model with liquid (*1*, *3* metal, *2* liquid)

free. Wave processes that occur in the fluid filling the pipe are considered as acoustic ones. The impedance boundary conditions at the edges of the pipe simulate infinite acoustic environment.

Additional information for the solution of the inverse problem of identification of the crack is ATRs of electric potentials at the free electrode sensors (Fig. 1b, c):

$$\begin{matrix} \varphi|_{s_1} = g_1(t) \\ \varphi|_{s_2} = g_2(t) \end{matrix} \quad t \in [0, t_2] \tag{2.39}$$

where s_1, s_2 are the free electrodes of sensors 1 and 2, respectively (Fig. 1).

The values of s_1, dr, γ are required to identify; they characterize the crack (Fig. 1a). The distance from the first sensor to crack s_1 is determined at the first step; the crack penetration depth dr perpendicular to the surface is determined at the second step. Identification of defects is carried out by using ANN. The direct nonstationary problem for the pipe segment is solved for ANN training (Fig. 1, right). Let dr is the penetration depth and γ is the angle of the semicircular crack on the external or internal surface of the pipe (Fig. 1, left). The geometric parameters of the pipe are length $h = 2$ m, inner radius $r = 0.19$ m, thickness $tr = 0.02$ m, the distance from the first piezosensor to the defect $s_1 = 0.5$ m, the distance from the defect to the edge of the pipe $l_1 = 0.5$ m, the distance from the piezoactuator to the second piezosensor $s_2 = 0.7$ m, and the distance from the second piezosensor to the edge of the pipe $l_2 = 0.3$ m. Axisymmetric finite element model is built in ANSYS for Young's modulus $E = 2.0 \times 10^{11}$ Pa, density $\rho = 7800$ kg/m^3, and Poisson's ratio $v = 0.3$.

Excitation of the waves is performed by setting potential difference on the electrodes of the piezoactuator with step-like time dependence (the duration of action is 1×10^{-6} s). The measured data are the ATRs of the electric potential at the free piezosensor electrode, located on the external surface of the pipe. There are two cases of its location: (i) near to the piezoactuator, and (ii) at a distance from it. We assume that a defect locates between actuator and sensor (Fig. 1). Measurement of the signal, reflected from defect, is produced in the time interval $[t_1, t_2]$. We assumed, that t_1 is the time, when a reflected signal reaches sensor, t_2 is the time, when the signal, reflected from the pipe edges, reaches sensor: $t_1 = 2s_1/v,\ t_2 = 2(s_1 + l_1)/v,\ \Delta t = t_2 - t_1$ (where v is the speed of the signal). For the second piezoelectric sensor, this interval is $t_1 = s_2/v,\ t_2 = (s_2 + 2l_2)/v,\ \Delta t = t_2 - t_1$.

3 Identification of Defects with the Use of Artificial Neural Networks

3.1 ANN Architecture

Multilayer network with back propagation is applied (Fig. 2). This architecture is perfectly suited for the task and combines the ease of implementation and performance.

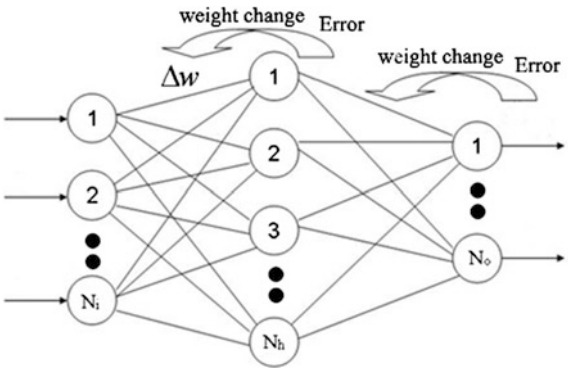

Fig. 2 Explanation of the back propagation

Two hundred data vectors were formed, 90% of which were used for training and 10% for testing. Then the computer experiments were performed using ANN.

The square error, er, for a particular network configuration is determined by providing a network of all existing observations (n) and comparing the actual output values with the desired (target) values:

$$\mathrm{er} = \frac{1}{2}\sum_{i=1}^{n}(d_i - y_i)^2, \tag{3.1}$$

where d is the desired network output; y is the real network output.

After training, the network can be used to predict output values. The accuracy of prediction is calculated according to the formula:

$$\mathrm{ex} = \frac{100}{N * M}\sum_{i=1}^{n}\sum_{j=1}^{m}\left(1 - \left|\frac{dt_{i,j} - yt_{i,j}}{dt_{i,j}}\right|\right), \tag{3.2}$$

where n is the number of samples for testing; m is the number of output data; dt is the desired network output at testing; and yt is the actual network output at testing.

3.2 The Processing of Input Data for ANN

Figure 3a presents ATR of electric potential φ, measured by piezoelectric sensor (curve 1 represents the data that correspond to the case of the pipe without defect; curve 2 represents the data that correspond to the case of the pipe with defect $dr = 5$ mm; curve 3 is the difference between 1 and 2). Moreover, the time interval used for ANN training is specified.

Case 1. The input data for the neural network is the ATR of φ per the period of time $[t_1, t_2]$, marked by a dotted line in Fig. 3a.

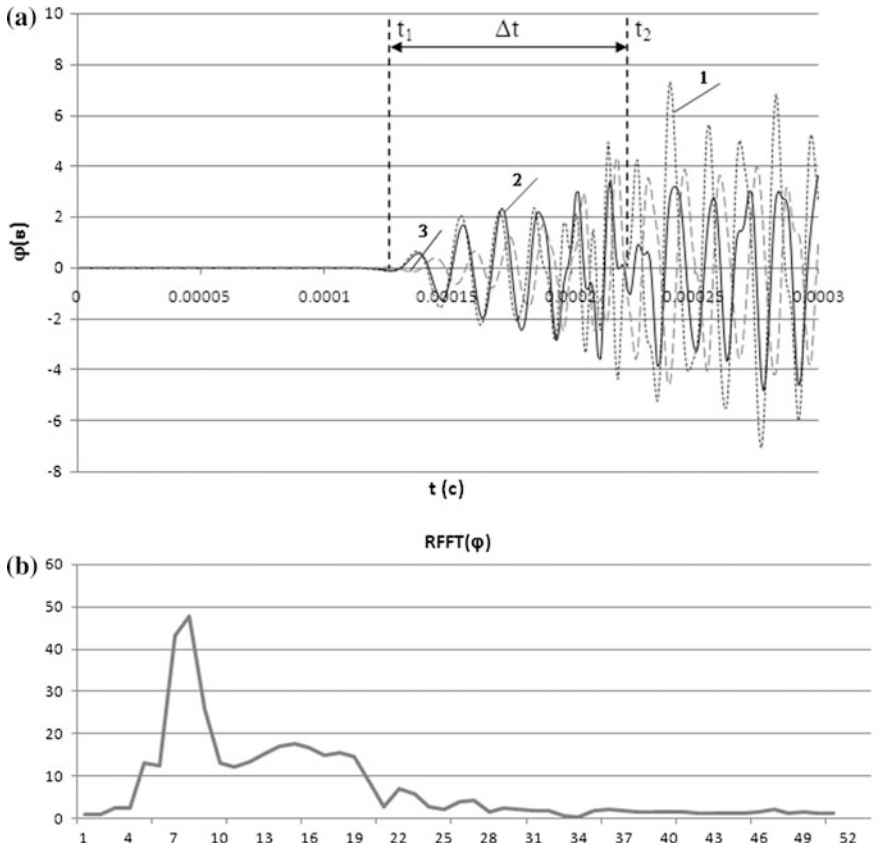

Fig. 3 **a** ATRs of electric potential φ for the pipe without the defect, with defect and their differences (input data for ANN correspond to case 1); **b** example of the ANN input data in case 2

Case 2. FFT algorithm is applied. Inputs to the neural network are values of the real parts of FFT (RFFT) (shown in Fig. 3b). In this case, the size of the input data decreases, so the training time will be less than in the first case.

4 Numerical Experiments

4.1 Determination of Distance to the Defect by Using Hardware

Figure 4 shows the difference between ATR of electric potential φ measured by the second piezosensor. Curve 1 represents the difference between φ for the empty pipe without defect and with it. Curve 2 represents the difference between φ of the pipe

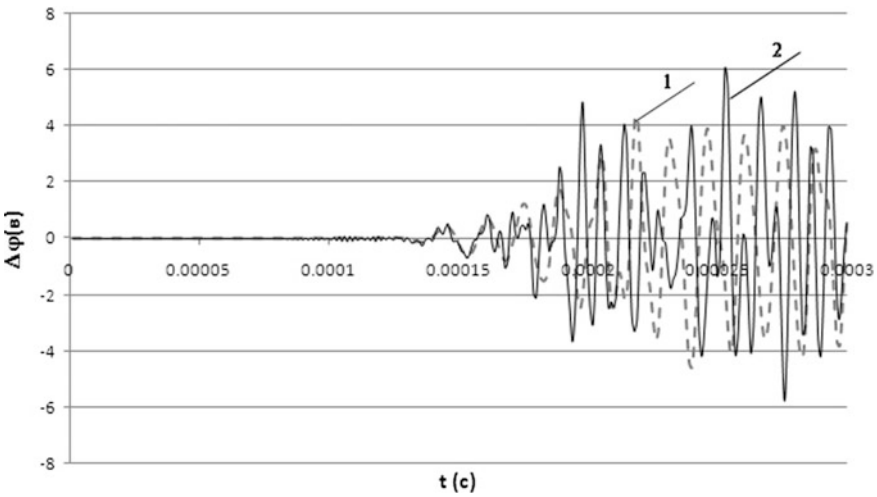

Fig. 4 Comparison of the difference between ATRs of the electric potential φ for the empty tube and the tube with the fluid

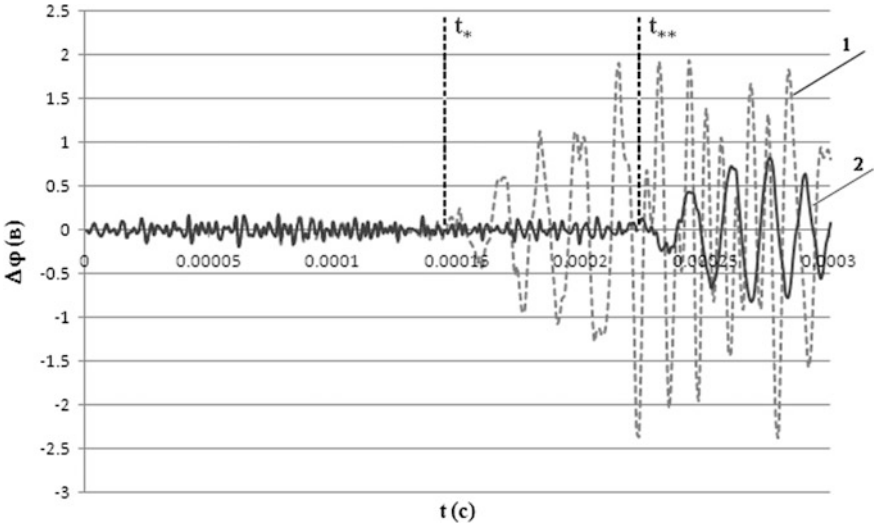

Fig. 5 Comparison of φ for the different defect positions

without defect filled with fluid and with the defect. The amplitudes and informative signal for empty pipe and filled with fluid are comparable, so further the ANN technology in the problem of identification of the defect is applied to an empty tube.

Figure 5 shows the difference between ATRs of electric potential φ measured by the first piezosensor. This case corresponds to an empty pipe with the different

distances s between the sensor and the defect. Curve 1 represents the difference between φ for the pipe without defect and with it on the external surface of the pipe. In the case of curve 1, $s_1 = 400$ mm. In the case of curve 2, $s_2 = 600$ mm. Using the time of arrival of the reflected signal t_* or t_{**}, we can estimate the distance to the defect. It is the first step in the identification of its parameters.

4.2 Determination of Distance to the Defect Using ANN

It was noted that the distance to the defect can be determined by using hardware according to the arrival time of the reflected signal. There is a possibility of the determination by using a trained neural network. It does not analyze the defect parameters, but identifies its location.

Table 1 shows the results of the identification of distance s to the defect by using ANN. The ANN structure is "200-20-1". It uses 2000 training iterations and 200 input vectors (180—training, 20—testing); we assume that $s \in [1300, 1700]$ mm. The defects locate on the outer surface of the pipe. The line number indicates the type of the defect in Table 2.

The data, presented in Table 1, show that the error of determining the distance value equals 5% for "small" defects and reduces to 1.5% for "large" defects.

4.3 Determination of Defect Parameters Using ANN

The second step is to determine the crack depth, which is defined from range $dr \in [0, 9]$ mm in a numerical experiment. The discussed defects are roughly divided into three classes (see Table 2). This separation can be associated with

Table 1 Results of the identification of the distance to defect

№	Depth of the defect (dr) (mm)	Accuracy of identification (%)
1	2	94.92
2	5	97.11
3	8	98.67

Table 2 Defect classes

№	The depth of the defect (dr) (mm)
1	0–3
2	3–6
3	6–9

classification of defects according to the degree of damage and the danger of the destruction of the pipe. For each class within the training and testing, we analyzed 200 defects.

The reconstruction of defect parameters was performed for two cases: (i) defects, located on the outer surface of the pipe; and (ii) defects, located on the inner surface of the pipe.

4.3.1 Reconstruction of Perpendicular Cracks

Let us first consider the crack perpendicular to the pipe surface. In this case, the depth of the defect, *dr*, shall be identified. Two hundred data vectors were formed, 90% of which were used for training and 10% for testing. Thereafter, the computer experiments are performed using the ANN. Error,er (Fig. 6), and prediction accuracy were defined by the formulae (3.1) and (3.2).

The results of the training and testing in the case of the second sensor are shown in Tables 3, 4, 5 and 6.

Table 3 shows the ANN structures, which give the best identification results, namely 51 input neurons, 10 hidden neurons, and one output neuron.

Table 4 shows that the best result is obtained with 2000 training iterations.

The results of training and testing in the Case 2, using the first sensor, are shown in Tables 7 and 8.

The results of Tables 5, 6, 7 and 8 listed in rows 1–3 correspond to Table 2.

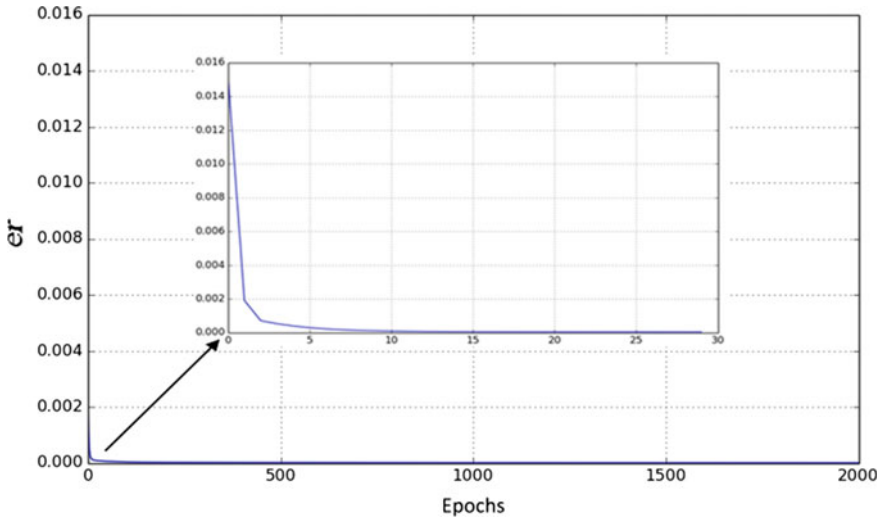

Fig. 6 Training error

Table 3 Results of training and testing ANN, using 2000 epochs and 200 input vectors (RFFT); different hidden layers are used and defects locate on the outer surface of the pipe

No.	ANN structure	Error (er)	Accuracy (ex) (%)
1	51-5-1	1.2×10^{-6}	99.58
2	**51-10-1**	$\mathbf{8.6 \times 10^{-7}}$	**99.67**
3	51-20-1	2.5×10^{-6}	99.22
4	51-30-1	1.9×10^{-5}	98.80
5	51-5-5-1	1.3×10^{-4}	96.97
6	**51-10-10-1**	$\mathbf{1.2 \times 10^{-6}}$	**99.43**
7	51-15-15-1	3.2×10^{-6}	99.17
8	51-20-20-1	3.5×10^{-6}	99.13

Table 4 Results of training and testing of ANN, using 200 input vectors (RFFT); different numbers of epochs are used and defects locate on the outer surface of the pipe

No.	ANN structure	Error (er)	Accuracy (ex) (%)
1	51-10-1	1000	99.37
2	**51-10-1**	**2000**	**99.67**
3	51-10-1	3000	99.46
4	51-10-1	4000	99.21

Table 5 Results of training and testing ANN using 2000 epochs; different values of the defect depth are used and defects locate on the outer surface of the pipe

No.	Amount of data	ANN structure	Error (er)	Accuracy (ex) (%)
1	200–all	100-20-1	2.1×10^{-6}	99.35
	200–RFFT	51-10-1	8.6×10^{-7}	99.67
2	200–all	100-20-1	3.8×10^{-6}	98.90
	200–RFFT	51-10-1	5.1×10^{-7}	99.64
3	200–all	100-20-1	3.5×10^{-6}	99.29
	200–RFFT	51-10-1	1.3×10^{-7}	99.87

Table 6 Results of training and testing ANN using 2000 epochs; different values of the defect depth are used and defects locate on the inner surface of the pipe

No.	Amount of data	ANN structure	Error (er)	Accuracy (ex) (%)
1	200–all	100-20-1	4.2×10^{-6}	99.24
	200–RFFT	51-10-1	6.1×10^{-6}	99.48
2	200–all	100-20-1	1.5×10^{-6}	99.71
	200–RFFT	51-10-1	7.0×10^{-7}	99.75
3	200–all	100-20-1	9.5×10^{-7}	99.70
	200–RFFT	51-10-1	9.8×10^{-7}	99.39

Table 7 Results of training and testing ANN using 2000 epochs; different values of the defect depth are used and defects locate on the outer surface of the pipe

No.	Amount of data	ANN structure	Error (er)	Accuracy (ex) (%)
1	200–all	100-20-1	8.4×10^{-6}	98.52
	200–RFFT	51-10-1	6.3×10^{-6}	98.62
2	200–all	100-20-1	2.7×10^{-6}	99.34
	200–RFFT	51-10-1	6.4×10^{-6}	99.07
3	200–all	100-20-1	7.7×10^{-7}	99.41
	200–RFFT	51-10-1	1.3×10^{-6}	99.27

Table 8 Results of training and testing ANN using 2000 epochs; different values of the defect depth are used and defects locate on the inner surface of the pipe

No.	Amount of data	ANN structure	Error (er)	Accuracy (ex) (%)
1	200–all	100-20-1	3.8×10^{-6}	98.95
	200–RFFT	51-10-1	6.5×10^{-6}	98.74
2	200–all	100-20-1	3.4×10^{-6}	99.26
	200–RFFT	51-10-1	4.1×10^{-6}	99.44
3	200–all	100-20-1	3.1×10^{-7}	99.68
	200–RFFT	51-10-1	2.5×10^{-7}	99.71

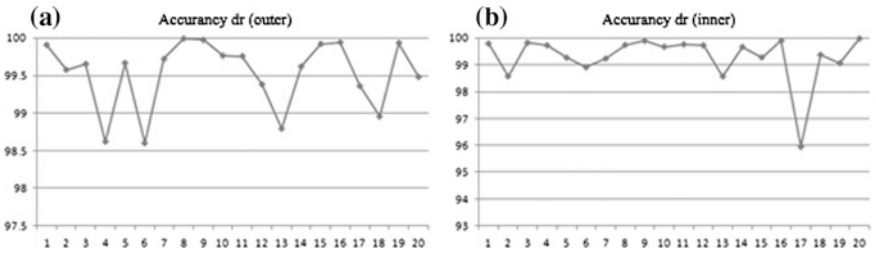

Fig. 7 Test results of identification of the defect depth

Figure 7 shows the test results of ANN (depth identification), displaying 20 examples with "10-01-51" architecture. The plots, shown in Fig. 7a, b, are built on the data, obtained by using the second row of Tables 5 and 6, respectively.

Figure 8 shows the results of identification in the case of using "noisy data" from formula (4.1). It is modeled the measurement error as

$$\breve{X}(t) = X(t) + \delta P(t)\mathrm{MAX}(|X(t)|), \tag{4.1}$$

where δ ranges from 1 to 10%, and $P(t)$ is the random variable uniformly distributed in the range $[-1, 1]$.

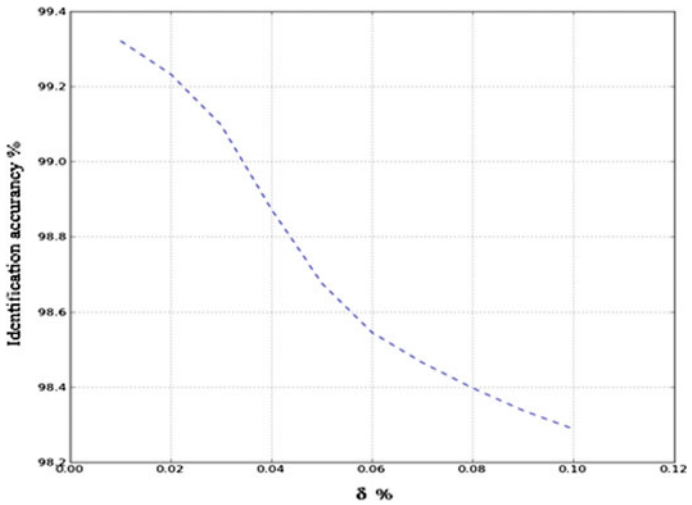

Fig. 8 Results of identification by using "noisy data"

Table 9 Results of training and testing ANN using 2000 epochs; different values of the defect depth and angle are used

No.	ANN structure	Error	Accuracy (%)	Sensor
1	100-10-2	0.0032	92.27	1
2	100-10-2	7.89×10^{-5}	95.95	1
3	100-10-2	0.3253	89.28	1
4	100-10-2	0.0119	97.39	2
5	100-10-2	3.91×10^{-5}	98.11	2
6	100-10-2	0.7315	84.47	2

4.3.2 Reconstruction of Inclined Cracks

In this section, we consider the identification of inclined cracks. Also as previously, defects are roughly divided into three classes (Table 2). We consider inclined cracks on the outer surface of the pipe. The inclination angle of the crack varies in the range [−45°; 45°]. Two hundred defects are used for each of the considered classes. The results of identification are shown in Tables 9, 10 and 11.

The numerical results showed that the identification error of inclined cracks does not exceed 10%. The architecture of trained ANN is 200-20-2 and 101-10-2. Thus, using the data, based on RFFT, accelerates more than two times speed of the learning process. For a more accurate reconstruction of defect parameters, the piezoelectric actuators and sensors, if it is possible in practice, should be located in the vicinity of the defect.

Table 10 Results of training and testing ANN using 2000 epochs; different values of the defect depth and angle are used

No.	ANN structure	Error	Accuracy (%)	Sensor
1	200-20-2	0.0024	95.32	1,2
2	200-20-2	1.48×10^{-5}	99.48	1,2
3	200-20-2	0.0146	92.52	1,2

Table 11 Results of training and testing ANN using 2000 epochs and 200 input vectors (RFFT); different values of the defect depth and angle are used

No.	ANN structure	Error	Accuracy (%)	Sensor
1	101-10-2	0.00059	96.75	1,2
2	101-10-2	8.71×10^{-6}	99.59	1,2
3	101-10-2	0.07695	92.19	1,2

5 Conclusion

In the result of this study, the method of the parameter identification of cracks on the outer or inner surface of the pipe, based on a combination of the finite element method and ANN, is developed. Additional information for the solution of the inverse problem of identification of the crack is ATRs of a radial and axial displacements and electric potential of piezosensor. This allows one to use the developed method in practice without complicated measurements. The study found that the preparation of the input data is the cornerstone in solving the problem. The most successful is the identification of the defect, based on the ATR, obtained by FFT. It is shown that the problem of identifying defects may be performed in two stages: (i) by determining the distance to the defect, and (ii) by determining its parameters.

Accuracy of determining the defect depth for the outer surface defect became 99.41 and 99.71% for the inner surface defect. Note that as additional information for the solution of inverse problems was used ATR of electrical potential of piezosensors, these sensors were located before the defect (for reflected signal) and after the defect (for passed signal). The results of numerical experiments showed that accuracy of the identification of defect parameters with trained ANN exceeded 95% at both locations of piezosensors. In the result of numerical experiments, we revealed ANN architectures that gave the best identification results, namely, 51 input neurons, 10 hidden neurons, and 1 output neuron.

In this architecture, we used the data, processed by the FFT. The size of input data was reduced, so the learning process became faster than in the case of using ATR data. Analysis of the input data showed that the ATR data could be used for identification defects in pipes, filled with fluid. The proposed identification algorithm was resistant to the error of input information.

Based on the foregoing, we conclude that the artificial neural network approach can be successfully used to identify defects on the surface of pipes by using the acoustic sensing of far field.

Acknowledgements This study for the first and third authors was supported by the Russian Science Foundation (Grant No. 17-08-00, 621).

References

1. S. Haykin, *Neural Networks: A Comprehensive Foundation* (John Wiley & Sons, NY, 1999), p. 823
2. A.A. Krasnoshchekov, B.V. Sobol', A.N. Soloviev, A.V. Cherpakov, Identification of defects crack-like defects in elastic structural elements on the basis of evolutionary algorithms. Russ. J. Non-destr. Testing **6**, 67 (2011)
3. P.S. Kurbatova, N.I. Saprunov, A.N. Soloviev, Use of neural networks in the task of determining defects in elastic bodies. in *Proceedings of X International Conference "Modern Problems of Continuum Mechanics"* (Southern Federal University Press, Rostov-on-Don, 2006), p. 75 (in Russian)
4. X. Fang, H. Luo, J. Tang, Structural damage detection using neural network with learning rate improvement. Comput. Struct. **83**(25), 2150 (2005)
5. V. Khandetsky, I. Antonyuk, Signal processing in defect detection using back-propagation neural networks. NDT and E Int. **35**(7), 483 (2002)
6. S.-W. Liu, J.-H. Huang, J.-C. Sung, C. Lee, Detection of cracks using neural networks and computational mechanics. Comput. Methods Appl. Mech. Eng. **191**(25), 2831 (2002)
7. Z. Waszczyszyn, L. Ziemiański, Neural networks in mechanics of structures and materials—new results and prospects of applications. Comput. Struct. **79**(22), 2261 (2001)
8. Y.G. Xu, G. Liu, Z. Wu, X. Huang, Adaptive multilayer perceptron networks for detection of cracks in anisotropic laminated plates. Int. J. Solids Struct. **38**(32), 5625 (2001)
9. A.O. Vatulyan, *Inverse Problems in Solid Mechanics* (Mir, Moscow, 2007), p. 224 (in Russian)
10. D.W. Kammler, *A First Course in Fourier Analysis* (Cambridge University Press, Cambridge, 2007)
11. V. Novatski, *Theory of Elasticity* (Mir, Moscow, 1975), p. 864
12. A.V. Belokon, A.V. Nasedkin, A.N. Soloviev, New scheme of the finite element dynamic analysis of piezoelectric devices. J. Appl. Math. and Mech. **66**(3), 491 (2002)